Applicability of hydrodynamics in relativistic heavy-ion collisions

Victor E. Ambruș

Physics Faculty, West University of Timișoara, Romania

Work in collaboration with C. Werthmann and S. Schlichting (U. Bielefeld)

arXiv:2211.14356 (PRL, in press); arXiv:2211.14379 [PRD, in press]

Wigner institute, Budapest, Hungary
03/04/2023

Outline

Quark-gluon plasma

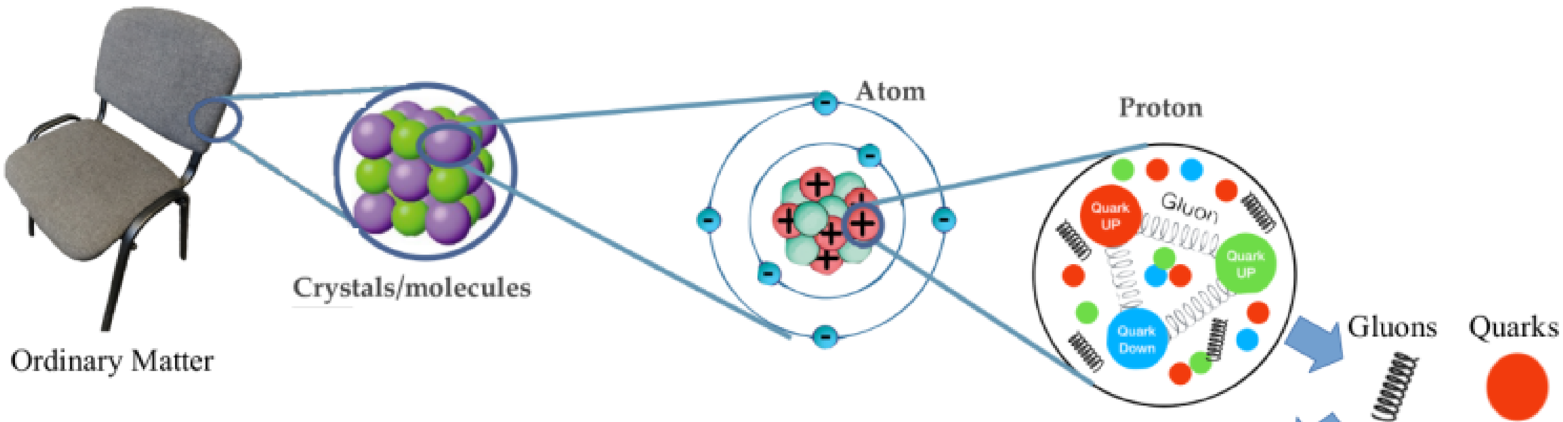

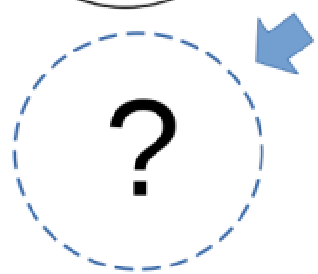

- Quarks are elementary particles interacting via the strong force, mediated by gluons.
- In normal conditions, they exist in bound, colour-neutral configurations (hadrons).
- In extreme conditions ($T \gtrsim 150$ MeV$/k_B \simeq 2 \times 10^{12}$ K), q and g become deconfined $\Rightarrow$ colour-neutral QGP with free colour charges.

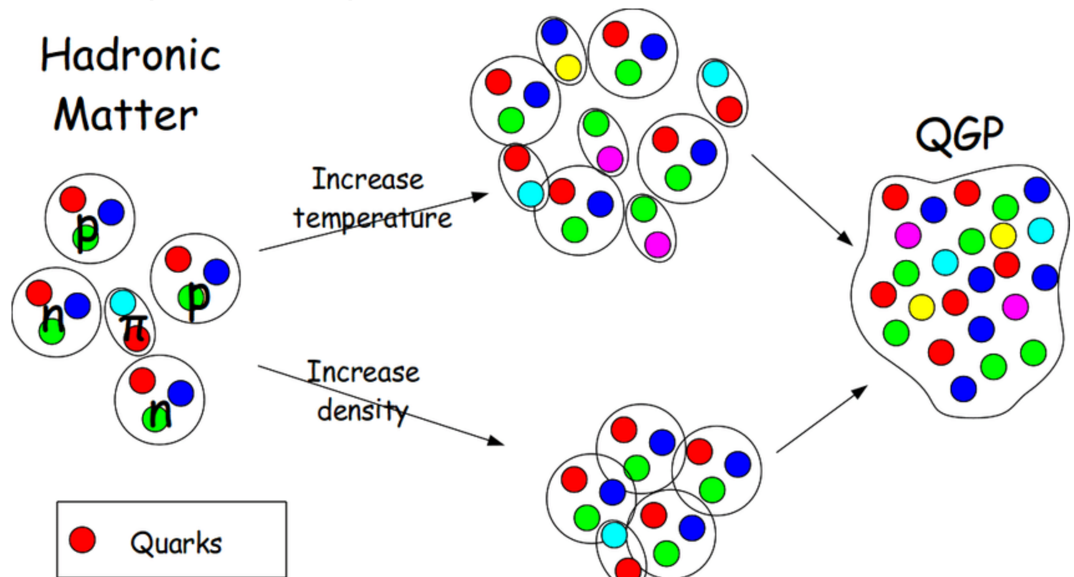

QGP in the laboratory

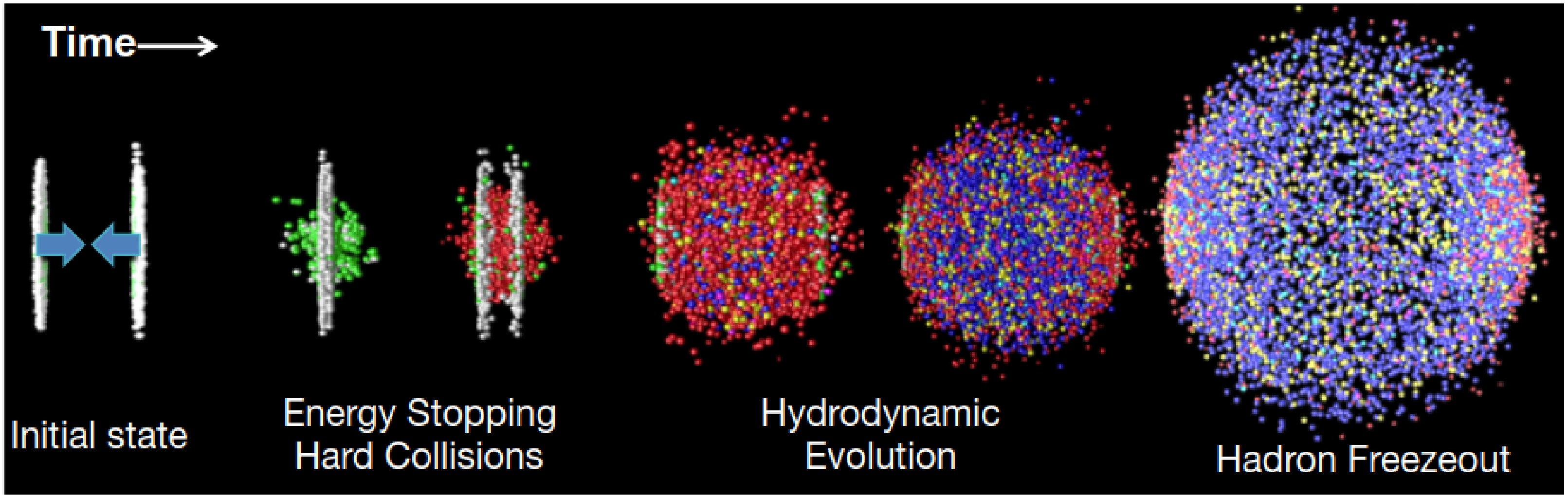

- Bjorken coordinates: $\tau = \sqrt{t^2 - z^2}$; $\eta = \tanh^{-1}(z/t)$.
- Ultra-relatistic heavy-ion collisions ($\sqrt{s_{NN}} = 5.02$ TeV PbPb) deposit $dE_{\perp}/d\eta \sim 1280$ GeV.
- Due to rapid longitudinal expansion, the QGP cools, reaching $k_B T \sim 350$ MeV at $\tau \simeq 1$ fm$/c$.

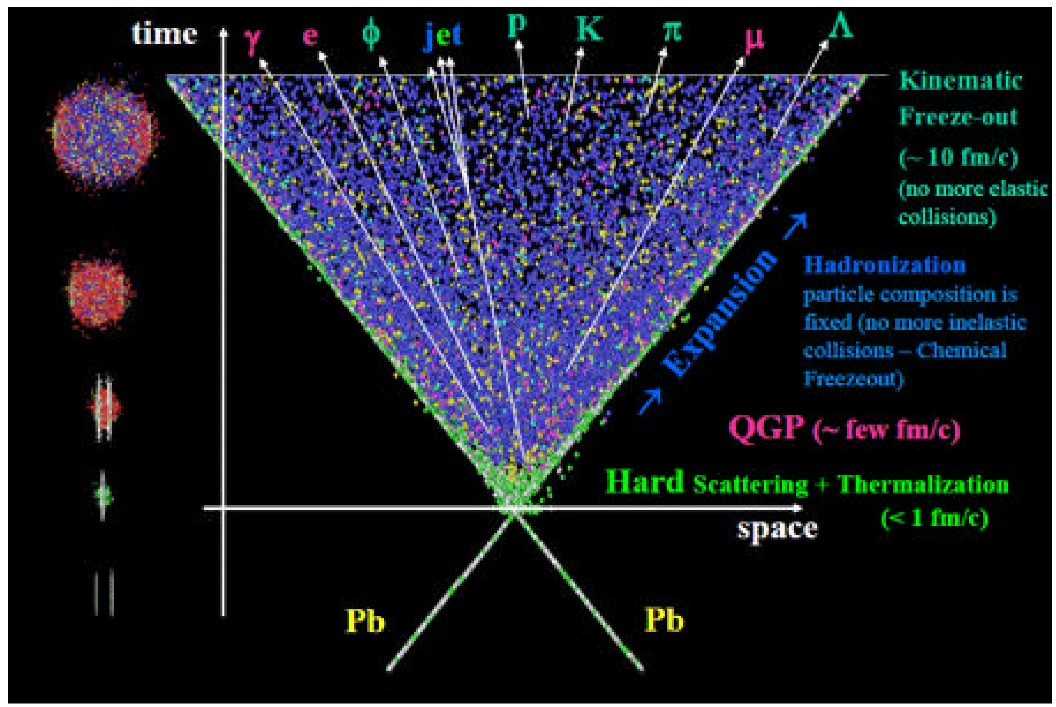

[Venaruzzo, PhD Thesis, 2011]

Transverse plane observables

- The overlap region between the colliding nuclei also expands in the transverse plane.
- The strong coupling of the QGP leads to hydrodynamic-like behaviour.
- Initial eccentricities ϵ_n lead to momentum-space anisotropies, characterized by flow harmonics v_n.
- $v_2 \equiv$ elliptic flow was one of the first exp. signatures for the formation of the QGP medium.

[CMS webpage]

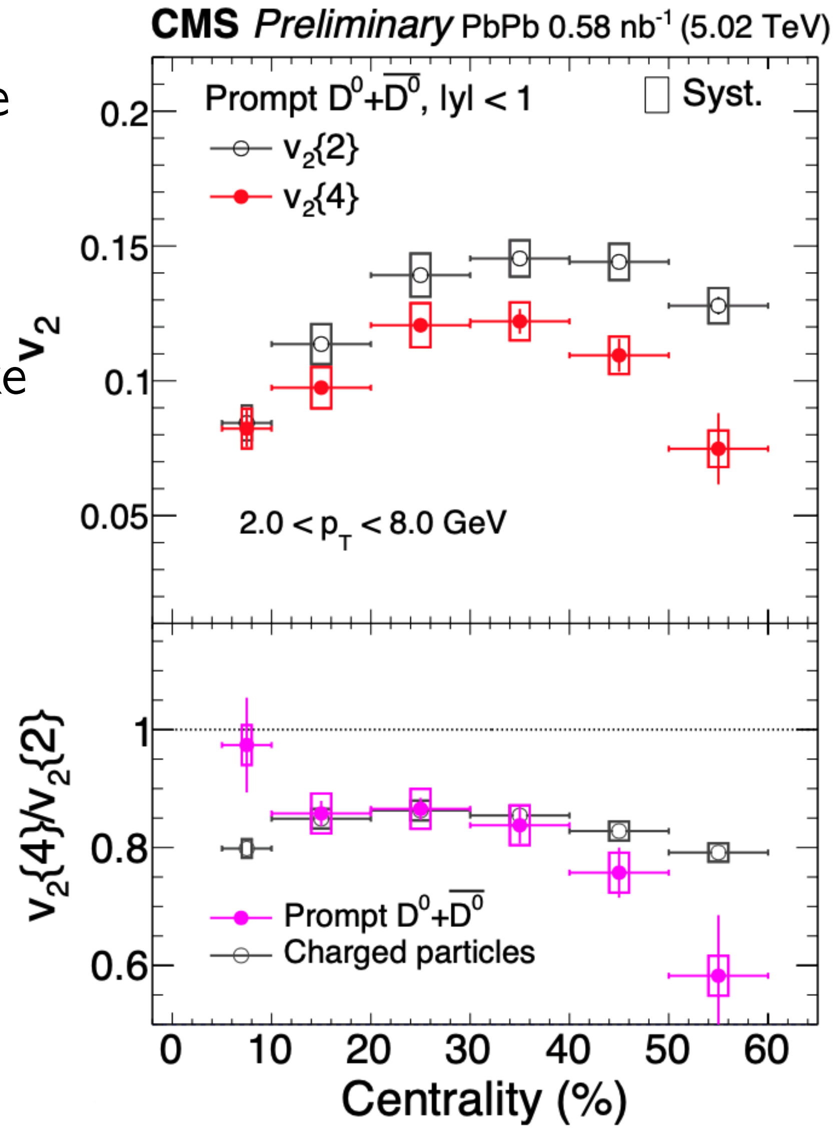

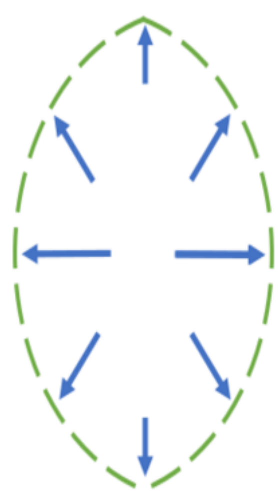

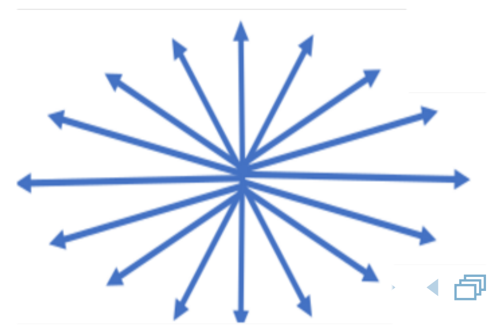

Aims of our Work

- Describe spacetime evolution of QCD fireball created in a hadronic collision
- Examine how pre-equilibrium dynamics affects final-state observables (energy $dE_\perp/dy$, Fourier coefficients v_n)
- small densities, large gradients: hydro not necessarily applicable; alternative: microscopic description in terms of kinetic theory
- numerical transport codes simulate these dynamics quite well

AMPT: He, Edmonds, Lin, Liu, Molnar, Wang [PLB 753 (2016) 506]

BAMPS: Greif, Greiner, Schenke, Schlichting, Xu [PRD 96 (2017) 091504]

- Employ simplified description in conformal kinetic theory and conformal hydro to understand the effects of pre-equilibrium dynamics on final-state observables in small and large systems.

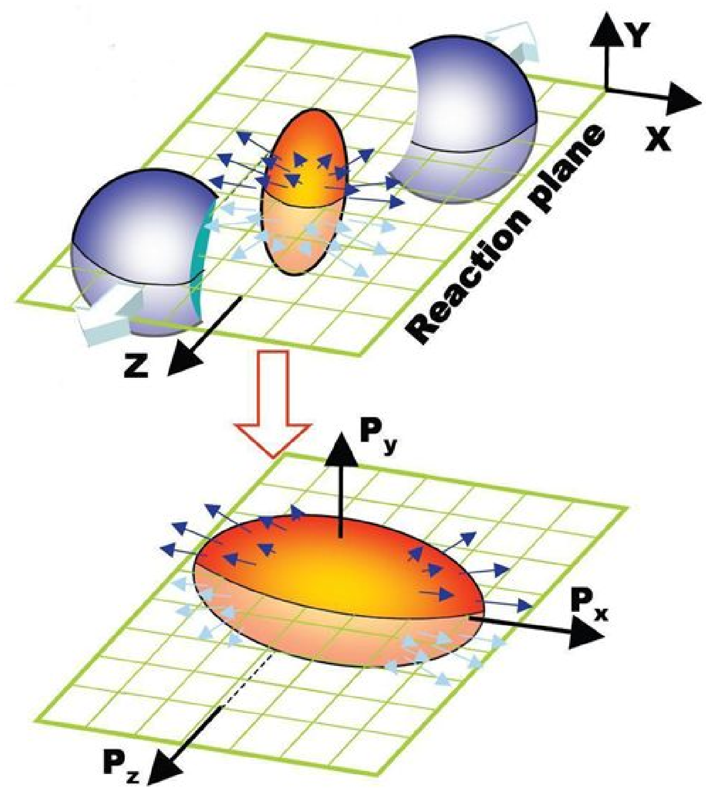

Hiroshi Masui (2008)

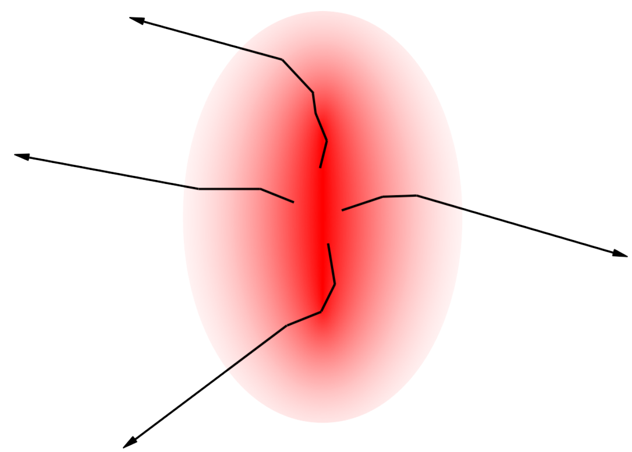

Microscopic description: Kinetic theory (RTA)

- We employ the averaged on-shell phase-space distribution f:

$$f(\tau, \mathbf{x}_\perp, \eta, \mathbf{p}_\perp, y) = \frac{(2\pi)^3}{\nu_{\rm eff}} \frac{dN}{d^3x\, d^3p}(\tau, \mathbf{x}_\perp, \eta, \mathbf{p}_\perp, y). \qquad (1)$$

- For simplicity, we assume boost invariance: $(2+1)+3$D description.
- Time evolution of f governed by Boltzmann eq. in RTA:

$$p^\mu \partial_\mu f = C_{RTA}[f] = -\frac{p_\mu u^\mu}{\tau_R}(f - f_{eq}), \qquad \tau_R = \frac{5\eta/s}{T}, \qquad (2)$$

where the specific shear viscosity $\eta/s \simeq \text{const}$.
- Numerical solution: Relativistic lattice Boltzmann (RLB) method.

[PRC 98 (2018) 035201; PRD 104 (2021) 094022; PRD 105 (2022) 014031]

Opacity

- For simplicity, we only consider energy-weighted dofs, characterizing the reduced distribution

$$\mathcal{F}(\tau, \mathbf{x}_\perp; \phi_p, v_z) = \frac{\nu_{\text{eff}}}{(2\pi)^3} \frac{\tau_0}{R\epsilon_{\text{ref}}} \int_0^\infty dp\, p^3 f, \tag{3}$$

  where $v_z = \tau p^\eta / p^\tau = \tanh(y - \eta)$ and $\phi_p = \arctan(p^y/p^x)$.

- Taking as reference energy $\epsilon_{\text{ref}} = \frac{1}{\pi R^3}(dE_\perp^0/d\eta)$ and length $\ell_{\text{ref}} = R$, with

$$\frac{dE_\perp^0}{d\eta} = \int d^2x_\perp \frac{dE_\perp^0}{d\eta d^2\mathbf{x}_\perp}, \quad R^2 \frac{dE_\perp^0}{d\eta} = \int d^2x_\perp \frac{dE_\perp^0}{d\eta d^2\mathbf{x}_\perp} x_\perp^2. \tag{4}$$

  $\mathcal{F}$ satisfies

$$\left(v^\mu \tilde{\partial}_\mu\right) \mathcal{F} = -\hat{\gamma}\, v^\mu u_\mu \tilde{T} \left(\mathcal{F} - \mathcal{F}_{eq}\right), \tag{5}$$

  where $\tilde{T} = T/T_{\text{ref}}$ and $T_{\text{ref}} = (\epsilon_{\text{ref}}/a)^{1/4}$.

- Once the initial state is specified (we consider $\tau_0 \to 0$), the system evolution is governed solely by the opacity:

$$\hat{\gamma} = \frac{RT_{\text{ref}}}{5\eta/s} = \frac{1}{5\eta/s} \left(\frac{R}{\pi a} \frac{dE_\perp^0}{d\eta}\right)^{1/4}. \tag{6}$$

Macroscopic description: Müller-Israel-Stewart hydro

- Writing $T^{\mu\nu} = (\epsilon + P)u^\mu u^\nu - P g^{\mu\nu} + \pi^{\mu\nu}$, $\partial_\mu T^{\mu\nu} = 0$ leads to

$$\dot{\epsilon} + (\epsilon + P)\theta - \pi^{\mu\nu}\sigma_{\mu\nu} = 0, \tag{7a}$$

$$(\epsilon + P)\dot{u}^\mu - \nabla^\mu P + \Delta^\mu{}_\lambda \partial_\nu \pi^{\lambda\nu} = 0, \tag{7b}$$

  where $\theta = \partial_\mu u^\mu$ and $\sigma_{\mu\nu} = \nabla_{\langle\mu} u_{\nu\rangle}$.
- In ideal hydro, $\pi^{\mu\nu} = 0$.
- In MIS viscous hydro, $\pi^{\mu\nu}$ evolves according to

$$\tau_\pi \dot{\pi}^{\langle\mu\nu\rangle} + \pi^{\mu\nu} = 2\eta\sigma^{\mu\nu} + 2\tau_\pi \pi_\lambda^{\langle\mu}\omega^{\nu\rangle\lambda} - \delta_{\pi\pi}\pi^{\mu\nu}\theta - \tau_{\pi\pi}\pi^{\lambda\langle\mu}\sigma_\lambda^{\nu\rangle} + \phi_7 \pi_\alpha^{\langle\mu}\pi^{\nu\rangle\alpha}, \tag{7c}$$

  where $\omega_{\mu\nu} = \frac{1}{2}[\nabla_\mu u_\nu - \nabla_\nu u_\mu]$ is the vorticity tensor.
- The transport coefficients are chosen for compatibility with RTA:

  [Ambruș, Molnár, Rischke, PRD **106** (2022) 076005]

$$\eta = \frac{4}{5}\tau_\pi P, \quad \delta_{\pi\pi} = \frac{4\tau_\pi}{3}, \quad \tau_{\pi\pi} = \frac{10\tau_\pi}{7}, \quad \phi_7 = 0, \quad \tau_\pi = \tau_R. \tag{7d}$$

- Numerical solution obtained using vHLLE.

[Karpenko, Huovinen, Bleicher, CPC 185 (2014) 3016]

Initial state $(\tau_0 \to 0)$

[Borghini, Borrell, Feld, Roch, Schlichting, Werthmann, arXiv: 2209.01176]

30-40% centrality:

Single event:

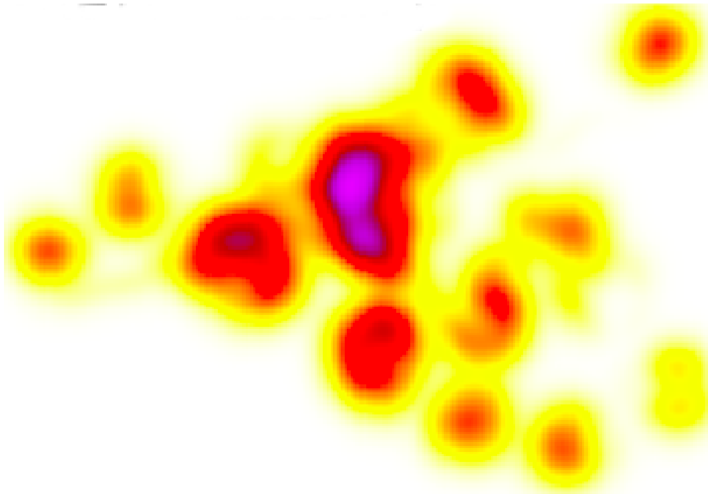

Averaged:

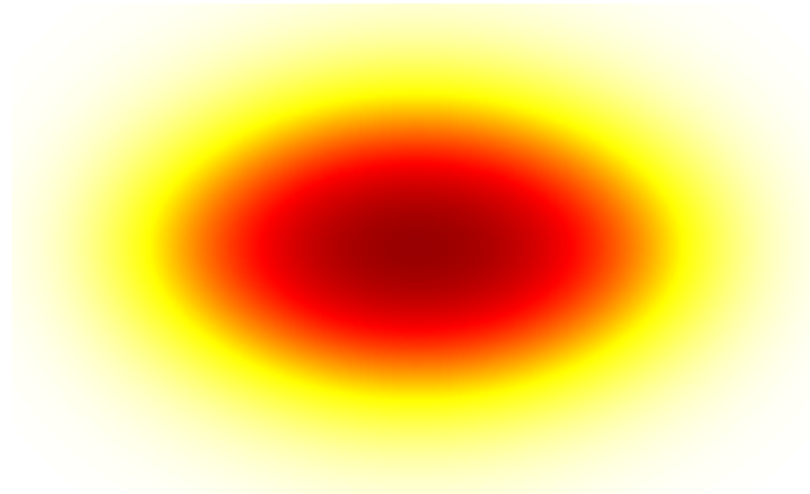

- We consider the initial $dE^0_\perp/d\eta d^2\mathbf{x}_\perp$ for averaged $30-40\%$ centrality PbPb collisions at $5.02\ \mathrm{TeV}$, characterized by

$$\frac{dE^0_\perp}{d\eta} = 1280\ \mathrm{GeV}, \qquad R = 2.78\ \mathrm{fm},$$

$$\epsilon_2 = 0.42, \quad \epsilon_4 = 0.21, \quad \epsilon_6 = 0.09. \tag{8}$$

Final-state observables ($\tau = 4R$)

- In order to facilitate the comparison between RTA and hydro, we choose final-state observables computable directly from $T^{\mu\nu}$.
- As a proxy for $dE_\perp/d\eta$, we consider

$$\frac{dE_{\mathrm{tr}}}{d\eta} = \tau \int_{\mathbf{x}_\perp} (T^{xx} + T^{yy}). \tag{9}$$

- Similarly, we characterize the flow ellipticity v_2 via

$$\varepsilon_p = \frac{\int_{\mathbf{x}_\perp} (T^{xx} - T^{yy} + 2iT^{xy})}{\int_{\mathbf{x}_\perp} (T^{xx} + T^{yy})}, \tag{10}$$

where Ψ_p is an event-plane angle.

Standard model of heavy-ion collisions

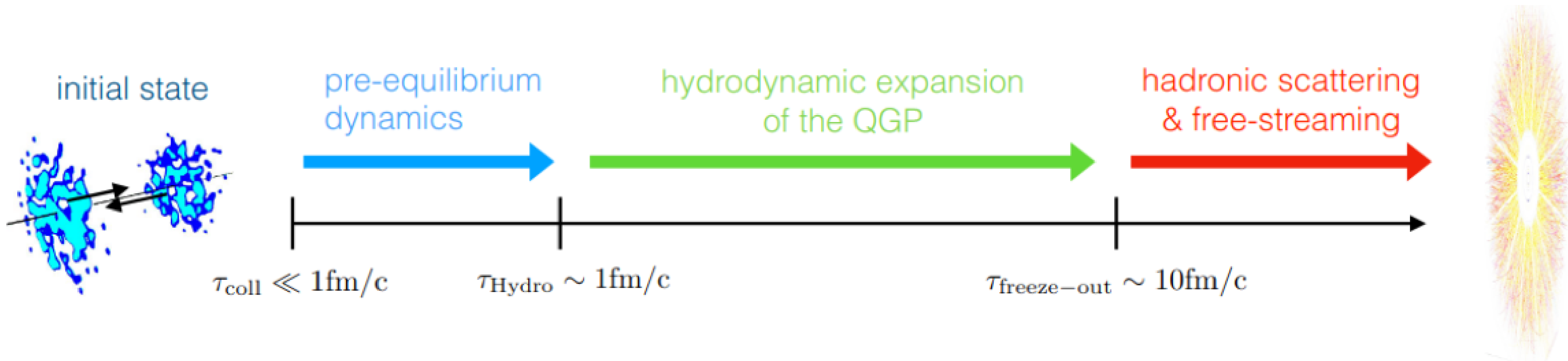

- $\tau_{\mathrm{coll}} \equiv \tau_0 \to 0$ to account for pre-eq. dynamics.
- Initially, the system is strongly off-equilibrium ($P_L \simeq 0$).

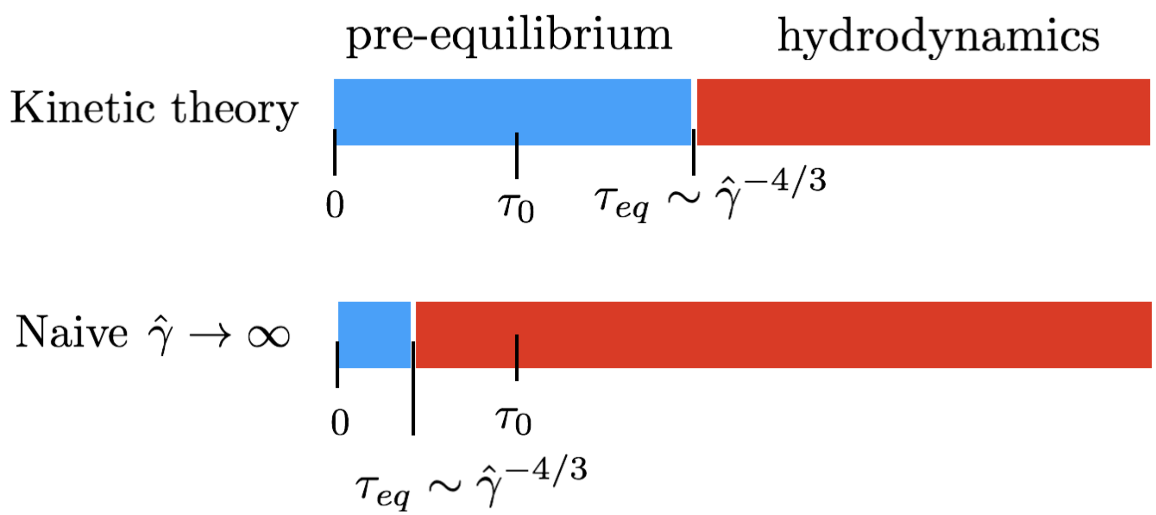

- If $\tau_{\mathrm{Hydro}} \equiv \tau_{\mathrm{eq}} \lesssim \tau_0$, the pre-eq. phase is not correctly modeled.
- Due to transverse structure, a new time scale R enters the picture
- If $\tau_{\mathrm{eq}} \gtrsim R$, equilibration is interrupted by transverse expansion and the system remains off-equilibrium throughout the evolution.

$0+1$-D Bjorken flow

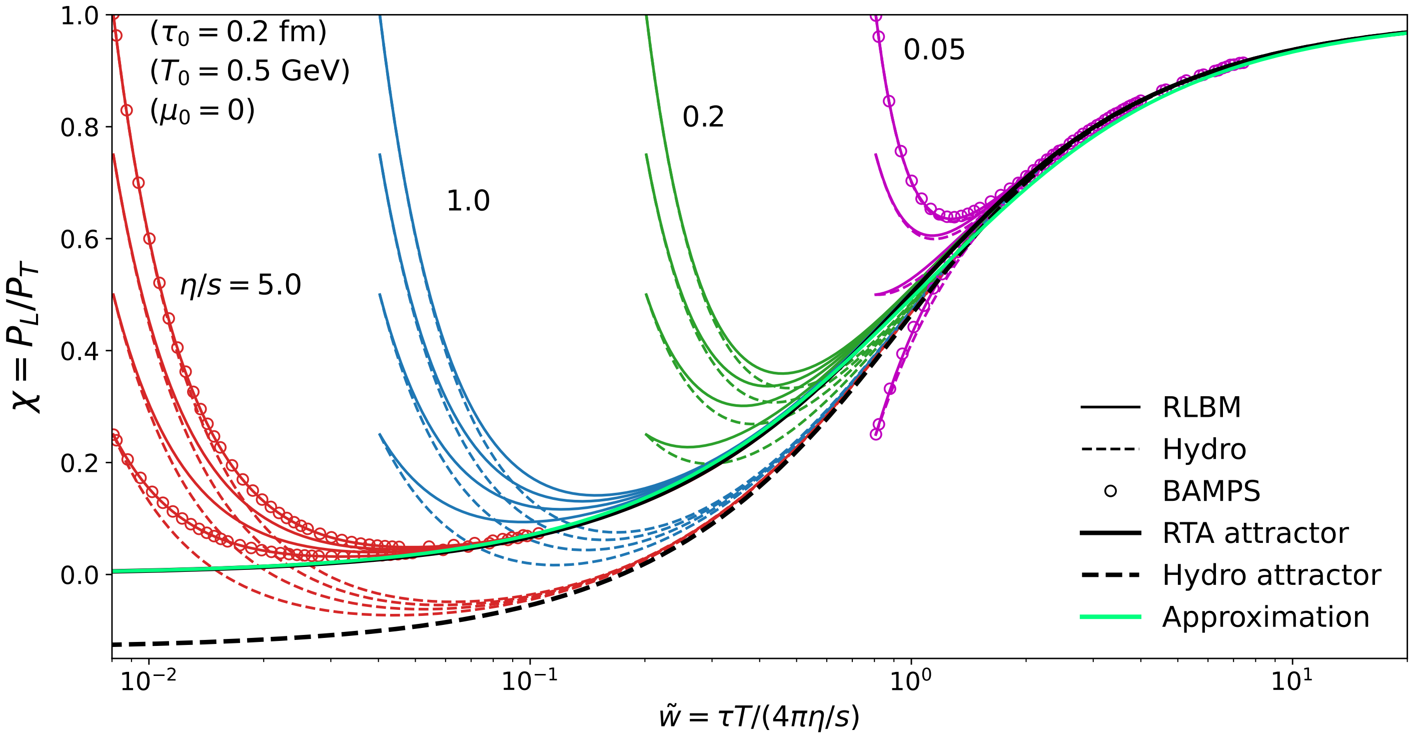

[Ambruș, Bazzanini, Gabbana, Simeoni, Succi, Nature Comput. Sci. **2**, 641 (2022)]

- At early times $\tau \ll R$, transverse expansion is negligible and

$$
\begin{aligned}
T^{\mu\nu} &\simeq \mathrm{diag}(\epsilon, \mathcal{P}_T, \mathcal{P}_T, \tau^{-2}\mathcal{P}_L), & \mathcal{P}_T &= P - \pi_d/2, \\
\pi^{\mu\nu} &\simeq \pi_d \mathrm{diag}(0, \tfrac{1}{2}, \tfrac{1}{2}, -\tau^{-2}), & \mathcal{P}_L &= P + \pi_d.
\end{aligned} \tag{11}
$$

- $f_\pi = \pi_d/\epsilon$ exhibits attractor behaviour. [Heller, Spaliński, PRL 115 (2015) 072501]

Pre-equilibrium dynamics: hydro perspective ($\tilde{w} \ll 1$)

- In MIS hydro, $f_\pi = \pi_d/\epsilon$ satisfies

$$\tilde{w}\left(\frac{2}{3} - \frac{f_\pi}{4}\right)\frac{df_\pi}{d\tilde{w}} + \frac{16}{45} + \left(\lambda - \frac{4}{3} + \frac{4\pi\tilde{w}}{5} - f_\pi\right) f_\pi = 0, \tag{12}$$

  where $\lambda = \frac{\delta_{\pi\pi}}{\tau_\pi} + \frac{\tau_{\pi\pi}}{3\tau_\pi} = 38/21$.

- Demanding regularity as $\tilde{w} \to 0$ reveals the attractor solution:

$$f(\tilde{w} \ll 1) = f_{\pi;0} + f_{\pi;1}\tilde{w} + \ldots, \tag{13}$$

  where

$$f_{\pi;0}^{\rm hydro} = \frac{1}{2}\left[\lambda - \frac{4}{3} - \sqrt{\left(\lambda - \frac{4}{3}\right)^2 + \frac{64}{45}}\right] = \frac{25 - 3\sqrt{505}}{105} \simeq -0.404,$$
$$f_{\pi;1}^{\rm hydro} = \frac{\frac{16\pi}{25} f_{\pi;0}^2}{(f_{\pi;0} - \frac{4}{15})^2 + \frac{16}{75}} \simeq 0.495. \tag{14}$$

- At early times, we have

$$\lim_{\tilde{w}\to 0} \frac{\mathcal{P}_L}{\mathcal{P}_T} = \frac{1 + 3f_\pi}{1 - \frac{3}{2}f_\pi} \simeq -0.13 < 0. \tag{15}$$

- In MIS hydro, $\mathcal{P}_L/\mathcal{P}_T$ casually descends below 0 as $\tau \to 0$.

Pre-equilibrium dynamics: RKT perspective

- In Bjorken flow, the Boltzmann equation admits the semianalytical solution

$$f(\tau, w, p_\perp) = D(\tau, \tau_0) f_0(w, p_\perp) + \int_{\tau_0}^{\tau} \frac{d\tau'}{\tau_R(\tau')} D(\tau, \tau') f^{\rm eq}(\tau', w, p_\perp), \tag{16}$$

where $w = \tau p v_z = \tau^2 p^\eta$ and $D(\tau_2, \tau_1) = \exp[-\int_{\tau_1}^{\tau_2} d\tau/\tau_R(\tau)]$.

- Eq. (16) allows ϵ and π_d to be expressed as

$$\epsilon = \frac{\tau_0 \epsilon_0}{\tau} D(\tilde{w}, \tilde{w}_0) + \frac{6\pi}{5} \int_{\tilde{w}_0}^{\tilde{w}} \frac{d\tilde{w}' D(\tilde{w}, \tilde{w}')}{1 - \frac{3}{8} f'_\pi} \frac{\epsilon'}{2} \mathcal{H}_\epsilon\left(\frac{\tau'}{\tau}\right),$$

$$\pi_d = -\frac{\tau_0 \epsilon_0}{3\tau} D(\tilde{w}, \tilde{w}_0) + \frac{6\pi}{5} \int_{\tilde{w}_0}^{\tilde{w}} \frac{d\tilde{w}' D(\tilde{w}, \tilde{w}')}{1 - \frac{3}{8} f'_\pi} \frac{\epsilon'}{2} \mathcal{H}_\pi\left(\frac{\tau'}{\tau}\right), \tag{17}$$

where

$$\mathcal{H}_\pi(y) = y^{7/3} \frac{d}{dy}\left(\frac{\mathcal{H}_\epsilon(y)}{y^{4/3}}\right), \quad \mathcal{H}_\epsilon(y) = y^2 + \frac{\arctan\sqrt{y^{-2} - 1}}{\sqrt{y^{-2} - 1}}. \tag{18}$$

- The coefficients in $f_\pi(\tilde{w} \ll 1) = f_{\pi;0} + f_{\pi;1}\tilde{w} + \dots$ read

$$f_{\pi;0} = -\frac{1}{3}, \quad f_{\pi;1} = \frac{4\pi}{5} - \frac{3}{4}\mathcal{I}_{\epsilon;1} \simeq 0.370, \quad \mathcal{I}_{\epsilon;1} = \frac{2\pi}{5}\int_0^1 \frac{dy}{y^{5/4}} \mathcal{H}_\epsilon(y). \tag{19}$$

- Naturally, $\mathcal{P}_L/\mathcal{P}_T \simeq 0$ when $\tilde{w} \to 0$.

Shear-stress attractor

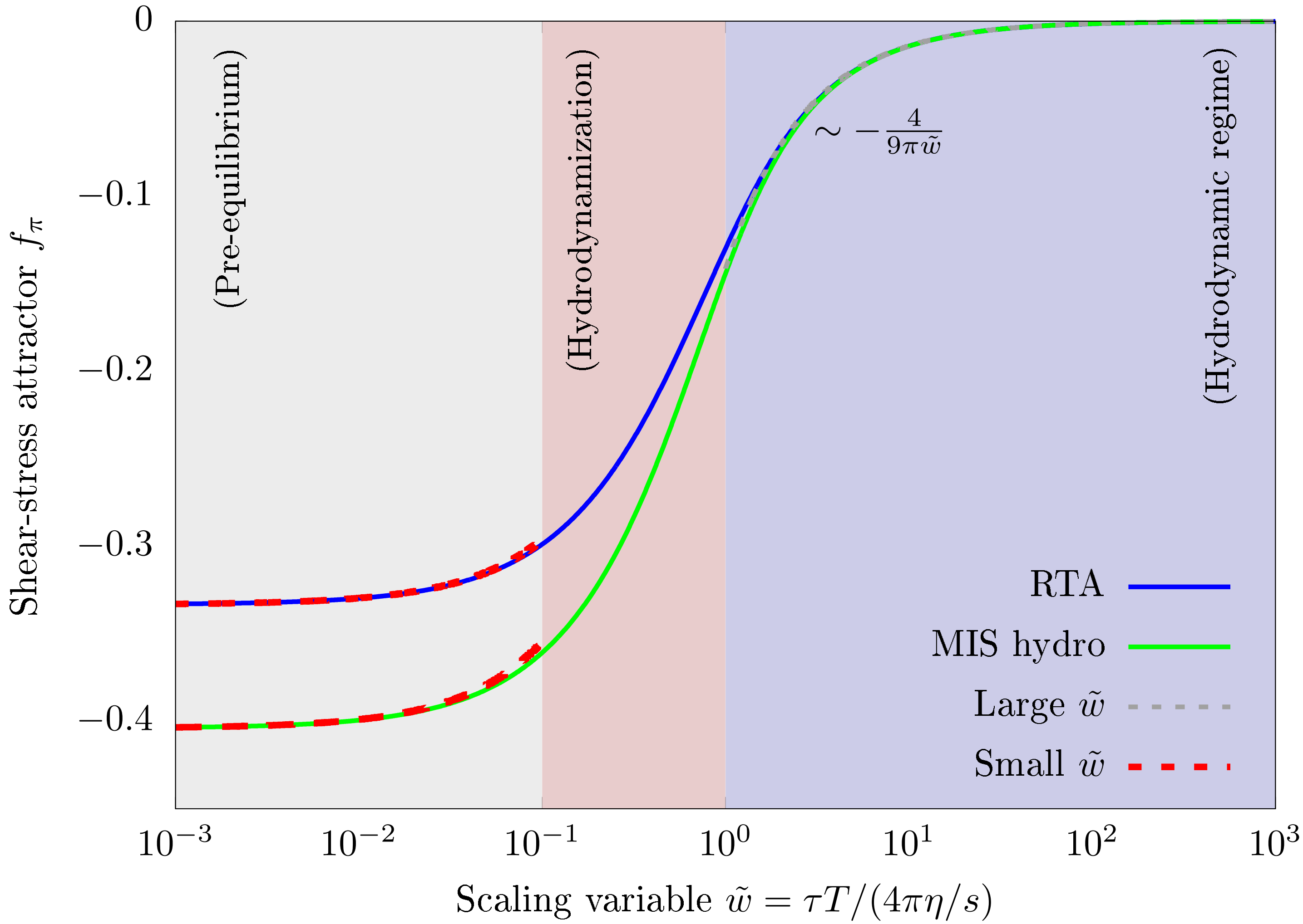

- f_π differs significantly in Hydro and RTA at small $\tilde{w}$.
- Agreement is reached when $\tilde{w} \gtrsim 1$, when

$$f_\pi(\tilde{w} \gg 1) = -\frac{4}{9\pi\tilde{w}} + O(\tilde{w}^{-2}). \tag{20}$$

Pre-equilibrium dynamics: Impact on energy

- The conservation of $T^{\mu\nu}$ leads to

$$\tau \frac{\partial \epsilon}{\partial \tau} + \frac{4}{3}\epsilon + \pi_d = 0. \tag{21}$$

- It is convenient to introduce the energy function $\mathcal{E}(\tilde{w})$,

$$\tau^{4/3}\epsilon(\tau) = \frac{\tau_0^{4/3}\epsilon_0}{\mathcal{E}(\tilde{w}_0)}\mathcal{E}(\tilde{w}) \qquad \Rightarrow \qquad \tilde{w}\left(\frac{2}{3} - \frac{f_\pi}{4}\right)\frac{d\mathcal{E}}{d\tilde{w}} + f_\pi \mathcal{E} = 0. \tag{22}$$

- Around $\tilde{w} = 0$, $\mathcal{E}$ behaves like

$$\begin{aligned} \mathcal{E}(\tilde{w} \ll 1) &\simeq C_\infty^{-1}\tilde{w}^\gamma(1 + \mathcal{E}_1\tilde{w} + \dots), & \gamma &= \frac{12 f_{\pi;0}}{3f_{\pi;0} - 8}, \\ \gamma_{\rm RTA} &= \frac{4}{9}, & C_\infty^{\rm RTA} &= 0.88, \\ \gamma_{\rm hydro} &= \frac{1}{18}(\sqrt{505} - 13) \simeq 0.526, & C_\infty^{\rm hydro} &= 0.82. \end{aligned} \tag{23}$$

- When Eq. (23) applies, we have

$$\epsilon(\tilde{w} \ll 1) \simeq \left(\frac{\tau_0}{\tau}\right)^{(\frac{4}{3}-\gamma)/(1-\gamma/4)}\epsilon_0 = \begin{cases} \frac{\tau_0}{\tau}\epsilon_0, & \text{(RTA)} \\ \left(\frac{\tau_0}{\tau}\right)^{0.93}\epsilon_0, & \text{(hydro)}. \end{cases} \tag{24}$$

- In RTA: $\tau\epsilon \simeq \mathrm{const.}$
- In hydro: $\tau\epsilon \propto \tau^{0.07}$ increases with time.

Energy attractor

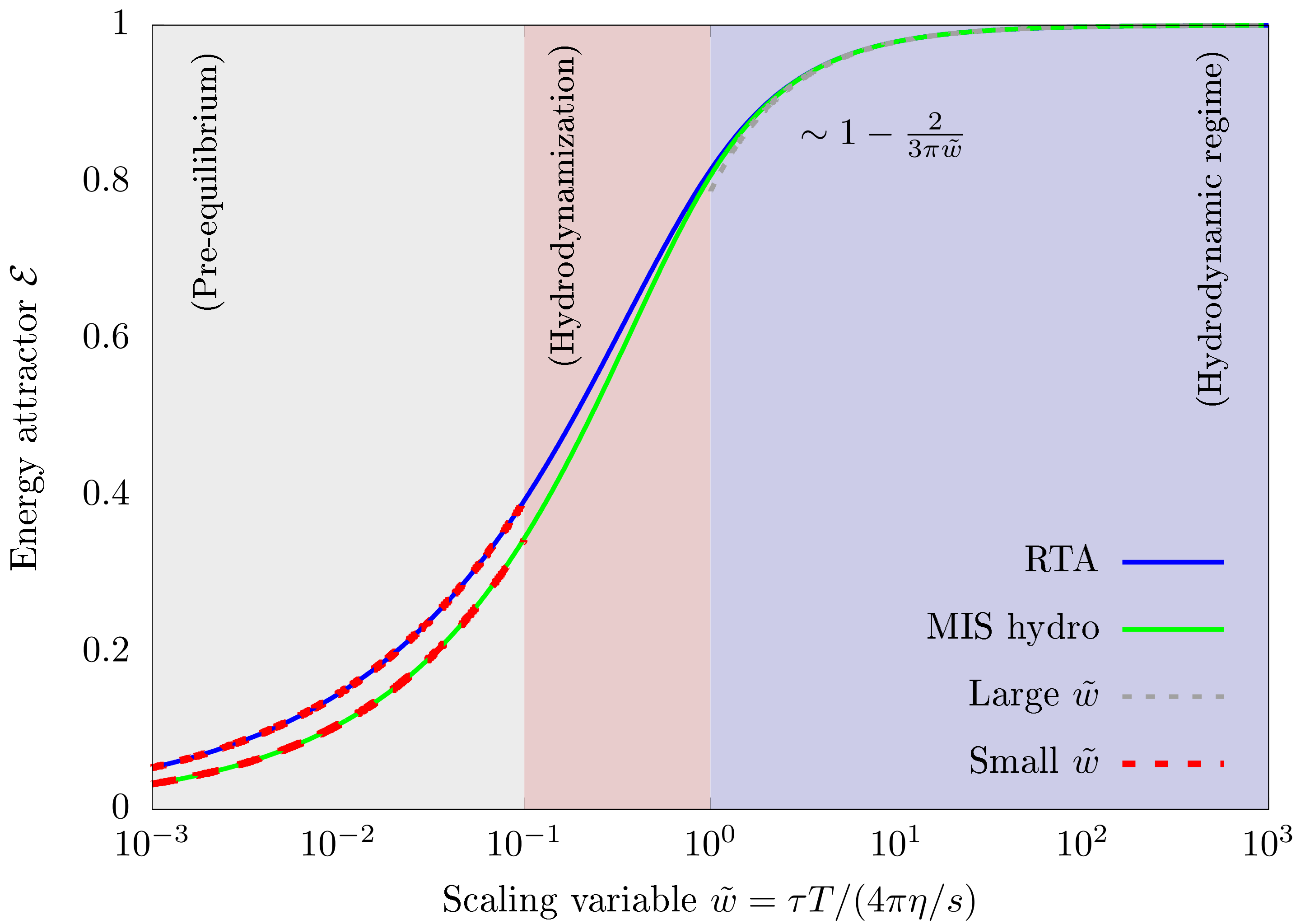

- $\mathcal{E}$ differs significantly in Hydro and RTA at small $\tilde{w}$.
- Agreement is reached when $\tilde{w} \gtrsim 1$, when

$$\mathcal{E}(\tilde{w} \gg 1) = 1 - \frac{2}{3\pi\tilde{w}} + O(\tilde{w}^{-2}). \tag{25}$$

Scaled hydrodynamics

- The hydro evolution of $\tau\epsilon$ is unphysical.
- At $\tilde{w} \gg 1$, hydro regains its validity.
- We scale hydro such that $(\tau^{4/3}\epsilon)_\infty^{\text{hydro}} = (\tau^{4/3}\epsilon)_\infty^{\text{RTA}}$:

$$C_\infty^{\text{hydro}} \frac{\epsilon_0^{\text{hydro}}}{\tilde{w}_0^{\gamma}} = C_\infty^{\text{RTA}} \frac{\epsilon_0^{\text{RTA}}}{\tilde{w}_0^{4/9}}.$$

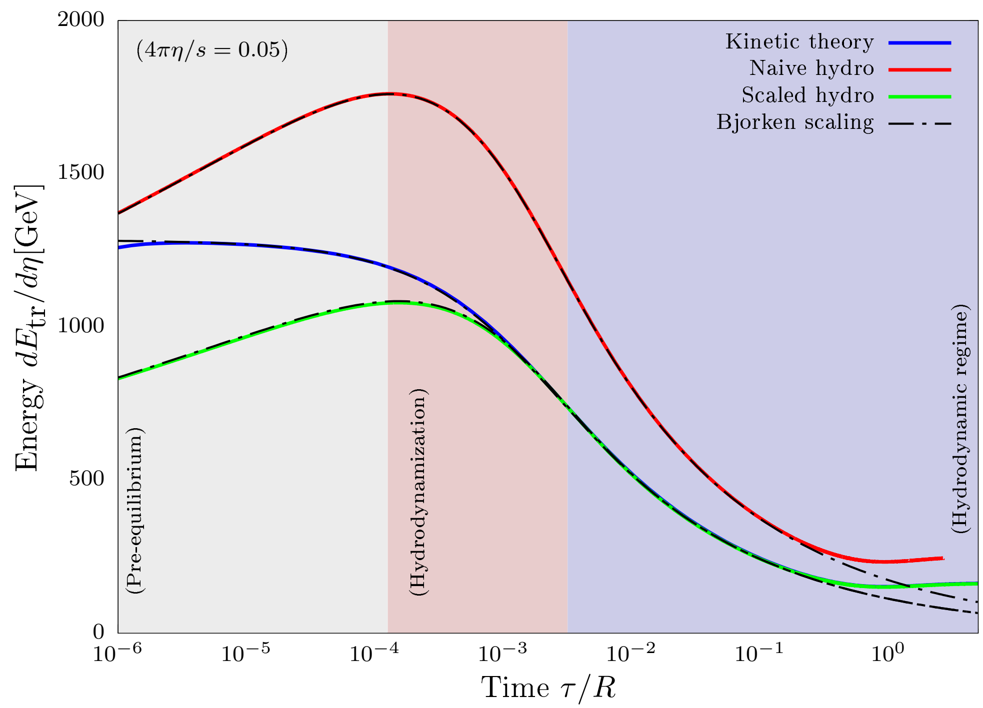

- Taking into account that $\tilde{w}_0 = \tau_0 T_0/(4\pi\eta/s)$ and $T_0 = (\epsilon_0/a)^{1/4}$, the solution is

$$\epsilon_0^{\text{hydro}} = \left[\left(\frac{4\pi\eta/s}{\tau_0} a^{1/4} \right)^{\frac{1}{2} - \frac{9\gamma}{8}} \left(\frac{C_\infty^{\text{RTA}}}{C_\infty^{\text{hydro}}} \right)^{9/8} \epsilon_0^{\text{RTA}} \right]^{\frac{8/9}{1-\gamma/4}}. \quad (26)$$

Final state ($\tau = 4R$): Transverse energy $dE_{\rm tr}/d\eta$

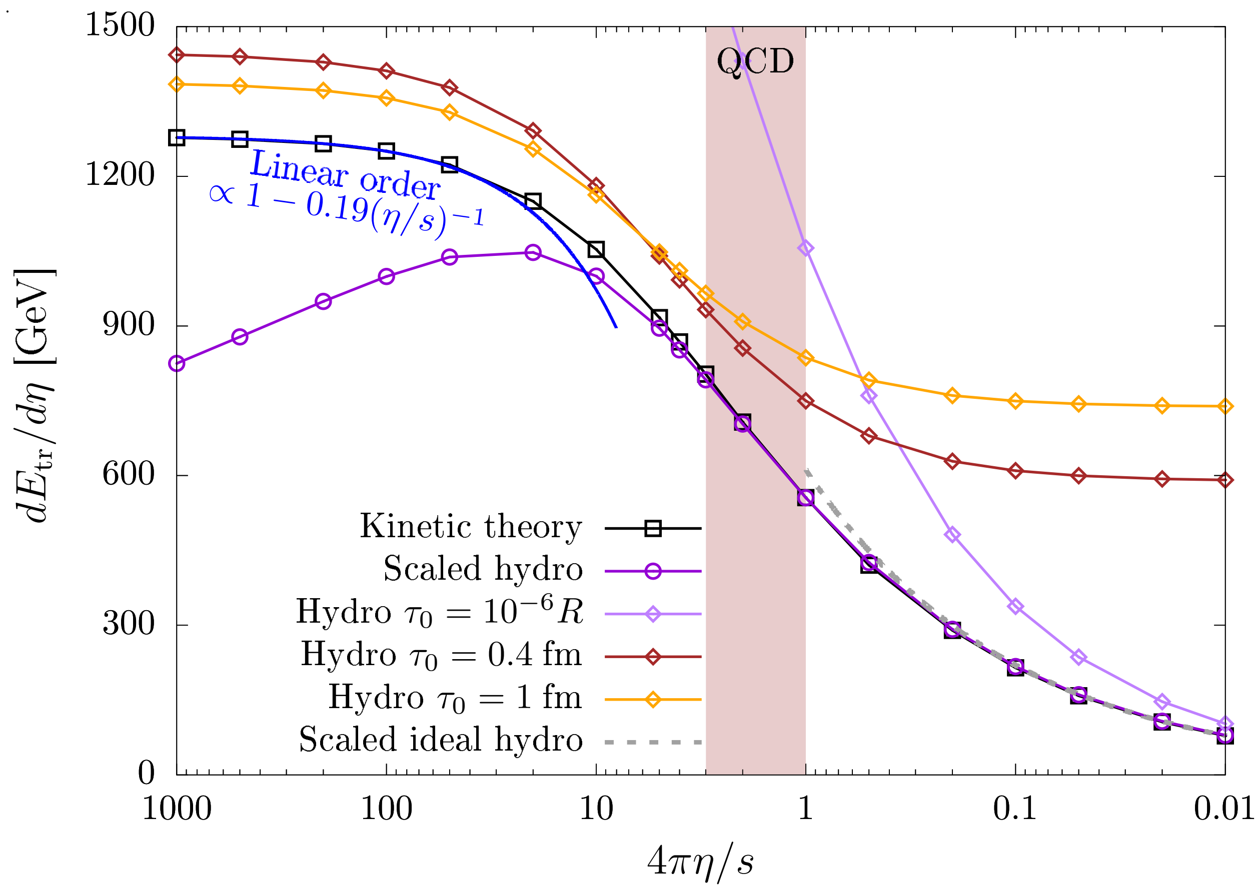

- [Naive hydro, small η/s] Larger $\tau_0 \Leftrightarrow$ larger final-state value, since late-time $dE_{\rm tr}/d\eta \propto \tau^{-1/3}$ decrease lasts less.
- [Naive hydro, large η/s] Smaller $\tau_0 \Leftrightarrow$ larger $dE_{\rm tr}/d\eta$ due to pre-eq. increase.
- [Scaled hydro, small η/s] Works well for $4\pi\eta/s \lesssim 3$.
- [Scaled hydro, large η/s] Transverse expansion interrupts pre-eq. $\Rightarrow dE_{\rm tr}/d\eta$ doesn't increase sufficiently to match RTA.

Inhomogeneous cooling and scaled eccentricity

- For $\tau \lesssim 0.1R$, the system evolves as a collection of $0+1$-D Bjorken flows $\Rightarrow$ inhomogeneous cooling.
- If $\tilde{w} \gtrsim 1$ when $\tau \sim R$, equilibration occurs before transverse expansion sets in and late-time limits governed by

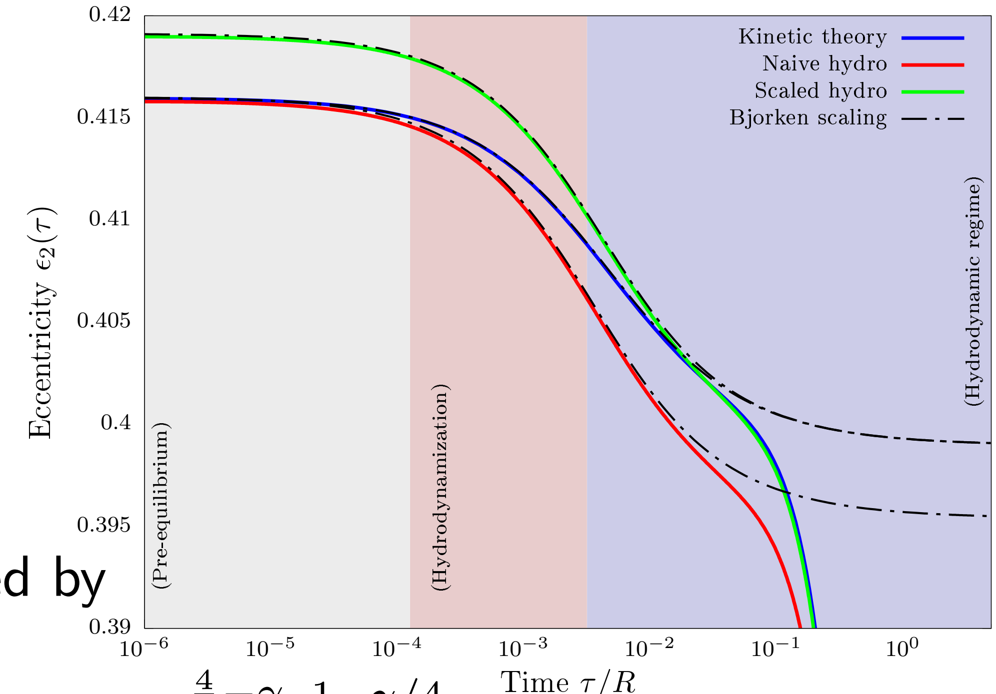

$$(\tau^{4/3}\epsilon)_\infty \propto \tau_0^{\frac{4}{3}-\gamma}\epsilon_0^{1-\gamma/4}. \tag{27}$$

- The eccentricity $\epsilon_2 = (\int_{\mathbf{x}_\perp}\epsilon)^{-1}\int_{\mathbf{x}_\perp}\epsilon x_\perp^2\cos(2\phi)$ changes according to

$$\epsilon_n \simeq \left(\int_{\mathbf{x}_\perp}\epsilon_0^{1-\gamma/4}\right)^{-1}\int_{\mathbf{x}_\perp}\epsilon_0^{1-\gamma/4}x_\perp^2\cos(2\phi). \tag{28}$$

- The exponent $1-\frac{\gamma}{4}$ implies that ϵ_2 changes differently in hydro compared to RTA $\Rightarrow$ scaled hydro changes initial ϵ_2 s.t. $\lim_{\tau\to\infty}\epsilon_2^{\text{hydro}} = \lim_{\tau\to\infty}\epsilon_2^{\text{RTA}}$.

Final state ($\tau = 4R$): Elliptic flow ε_p

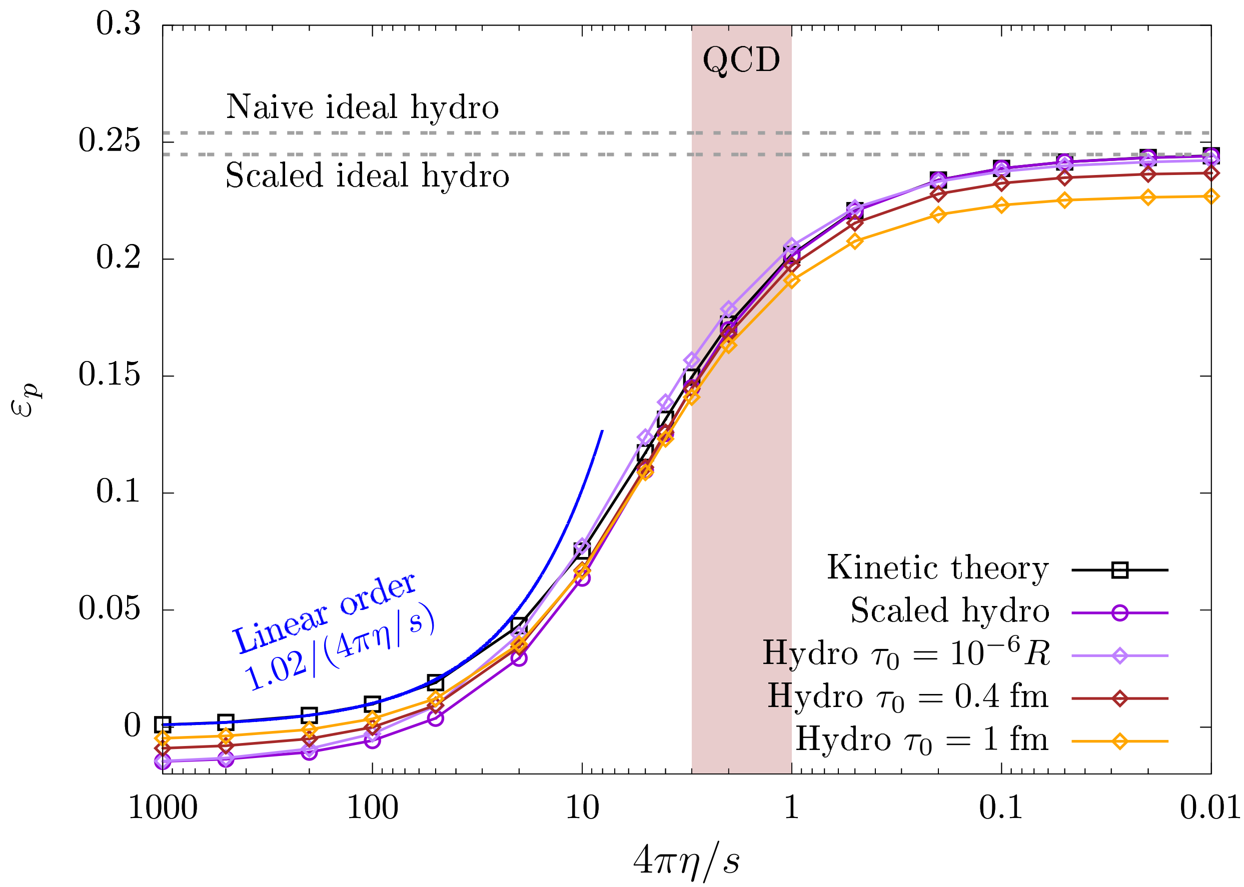

- [Naive hydro, small η/s] Remains in disagreement with naive ideal hydro. Approach to RTA: lucky coincidence?
- [Scaled hydro, small η/s] In excellent agreement with scaled ideal hydro & RTA.
- [Hydro, large η/s] Pre-equilibrium in hydro leads to negative build-up of ε_p (less for larger τ_0), which persists at late times (in contrast to RTA).

Conclusions

- During pre-equilibrium, hydro leads to an increase of $dE_\perp/dy \Rightarrow$ (severe) discrepancies in late-time $dE_\perp/dy$ in the $\tau_0 \to 0$ limit.
- Preeq. inhomogeneous cooling leads to different ϵ_n in RKT and hydro $\Rightarrow$ discrepancies in late-time ε_p.
- Bjorken $0+1$-D attractor governs the evolution for $\tau \lesssim 0.1R$.
- Hydro i.c.'s can be rescaled based on attractor $\Rightarrow$ late-time agreement with RTA. [works only for small η/s = large $\hat{\gamma}$!]
- For the sample $30-40\%$ centrality class of $\mathrm{Pb}-\mathrm{Pb}$ collisions at $\sqrt{s_{NN}} = 5.02\ \mathrm{TeV}$, scaled hydro provides a reasonable description when $4\pi\eta/s \lesssim 3$.
- Possible improvements include hybrid schemes: kinetic theory for pre-equilibrium and equilibration and hydro for the rest.
- This work was supported through a grant of the Ministry of Research, Innovation and Digitization, CNCS - UEFISCDI, project number PN-III-P1-1.1-TE-2021-1707, within PNCDI III.